

Effects of Manganese Addition on the Electronic Structure of BaTiO_3

J. F. Nossa,¹ Ivan I. Naumov,¹ and R. E. Cohen^{1,2}

¹*Geophysical Laboratory, Carnegie Institution of Washington, Washington D.C. 20015, USA*

²*Department of Earth Sciences, University College London,
Gower Street, WC1E 6BT, London, United Kingdom*

(Dated: December 24, 2014)

Abstract

Mn is used as a dopant to improve the electromechanical properties of perovskite oxides. We elucidate the role of Mn defects and associated vacancies on the electronic, atomic and ferroelectric properties of BaTiO_3 . Using density functional theory (DFT) and DFT+U we investigate the equilibrium geometry and electronic properties of Mn ion on A or B sites and with compensating oxygen vacancies. We study the change in the oxidation state of Mn in response to local environment changes, such as the presence of oxygen vacancies.

PACS numbers: 77.80.-e, 75.85.+t, 61.72.-y

Transition metal dopants improve the electromechanical properties of compounds like BaTiO₃, PbTiO₃ or PbZr_xTi_{1-x}O₃ (PZT),¹⁻⁹ but the origins of these effects are not well understood. Effects of the dopants can be divided into two categories, extrinsic and intrinsic. Extrinsic effects are mainly attributed to pinning of domain walls by the dopant ions and any associated oxygen vacancies. The intrinsic effects are not directly connected with domain boundary movement. They manifest themselves through the interaction between the doping induced local polarization \mathbf{P}_d and the spontaneous polarization \mathbf{P}_s . It has been proposed that the defective dipoles can cooperatively align along a certain crystallographic direction, producing a macroscopically observable internal bias field.^{5,6} One interesting intrinsic effect discussed in the literature is the possibility to increase the piezoelectric coefficients typical for PZT and Pb(Mg_{1/3}Nb_{2/3})_{1-x}Ti_xO₃ (PMN-PT) by a factor of 10-40.⁷ This phenomenon has also been observed in aged BaTiO₃ samples doped with Mn.^{8,9}

Among the dopants, Mn is special because it is magnetic and exhibits a variety of oxidation states (Mn²⁺, Mn³⁺ and Mn⁴⁺, and more). According to electron-spin-resonance (ESR) experiments, in ABO₃ perovskites, Mn forms neutral defects and goes in the A site as Mn²⁺, in the B site as Mn⁴⁺ or as Mn²⁺ with the formation of a charge compensation complex Mn²⁺-V_O²⁻.¹⁰⁻¹⁴ In terms of Kröger-Vink notation these defects can be denoted as Mn_A[×], Mn_B[×] and (Mn_B^{''}-V_O^{••})[×], respectively, where the symbol × stands for the neutral case, / for the net negative charge, and • for net positive charge relative to a defect-free host. When doped with Mn, the incipient ferroelectrics SrTiO₃ and KTaO₃ exhibit simultaneous spin and dipole glass behaviors with large non-linear magnetoelectric coupling.^{12,15-17} Such multiglass systems have attracted considerable attention because they can be viewed as a new class of multiferroics.

In contrast to SrTiO₃ and KTaO₃, ferroelectric BaTiO₃ doped with a 3d transition metal becomes multiferroic. This was shown theoretically within the framework of the local spin-density approximation (LSDA) and experimentally by magnetization measurements.^{18,19} The ferroelectric and magnetic ordering in such 3d-metal-doped BaTiO₃ multiferroics actually compete with each other, as demonstrated in Ref. 20 by studying BaTiO₃:Mn thin films. It was found that only films with a large amount of oxygen vacancies exhibit room-temperature ferromagnetic behaviour, and which was attributed to the formation of bound magnetic polarons.²¹

We briefly review some previous work on first-principles theory of defects in oxide ferro-

electrics: Yao and Fu studied the formation energies of different types of vacancies in PbTiO_3 as a function of (i) the Fermi level and (ii) chemical potentials of the atomic reservoirs.²² Cockayne and Burton computed the dipole moment of the $\text{V}_\text{O}^{\bullet\bullet}-\text{V}_\text{B}''$ divacancy and found that this moment can be twice as large as the dipole moment per cell of the bulk PbTiO_3 ; such defects, therefore, can be considered as an important source of local polarization and local fields.²³ He and Vanderbilt studied the pinning of domain walls via vacancies and revealed that the pinning effect can be strong.²⁴ Meštrić *et al.* investigated Fe^{3+} centers in PbTiO_3 and found that such centers tend to replace Ti^{4+} as acceptors and form charged defective associates $(\text{Fe}'_\text{A}-\text{V}_\text{O}^{\bullet\bullet})^\bullet$.²⁵ The orientation of the $(\text{Fe}'_\text{Ti}-\text{V}_\text{O}^{\bullet\bullet})^\bullet$ defective dipole was found to be along the c -axis parallel to the spontaneous polarization. DFT calculations for Cu impurities in PbTiO_3 found them to behave similarly to their counterpart Fe acceptor centers.²⁶ When isolated, their most stable charge state is Cu''_Ti , which leads to two holes in the valence band. Like Fe, the Cu centers have strong chemical driving force for association with oxygen vacancies to form $(\text{Cu}''_\text{Ti}-\text{V}_\text{O}^{\bullet\bullet})^\times$ defective dipoles whose preferable orientation is again along the $[001]$ axis.²⁶ Zhang *et al.* explored the effects of acceptor substitutes to the Ti site in PbTiO_3 .²⁷ They screened group IIIB and VB elements and found that these elements favor immobile acceptor-oxygen-vacancy-acceptor defect clusters. Moreover, they found that groups IIIB and VB dopants take two distinct defect-cluster structures along the z -direction and in the xy -plane, respectively. While the former enforces the domain pinning, the latter makes the domain pinning effects weaker.

Kvyatkovskii investigated the geometry and electronic structure for defects produced by the Mn impurities both in SrTiO_3 and KTaO_3 .^{28,29} He used a cluster approach where the crystalline environment of the defect is modeled by a cluster that is passivated by hydrogen atoms. Kondakova *et al.* in their local spin density approximation (LSDA) calculations showed that a Mn ion substituting for Sr in SrTiO_3 occupies the off-central position.³⁰ This result supports the idea that the observed dielectric anomalies in $\text{Sr}_{1-x}\text{Ti}_x\text{O}_3$ are due to motion of dipoles associated with the off-centered Mn^{2+} impurities.¹² Using LSDA+U and many-body perturbation theory, Kizian *et al.* calculated magnetic interactions in doped SrTiO_3 between the Mn impurities of different kinds: $\text{Mn}^{2+}_\text{Sr}-\text{Mn}^{2+}_\text{Sr}$, $\text{Mn}^{2+}_\text{Sr}-\text{Mn}^{4+}_\text{Ti}$ and $\text{Mn}^{4+}_\text{Ti}-\text{Mn}^{4+}_\text{Ti}$.³¹ They found that the exchange interaction between Mn^{2+}_Sr impurities is significantly smaller than those for Mn^{4+}_Ti and $\text{Mn}^{4+}_\text{Ti}-\text{Mn}^{4+}_\text{Ti}$ pairs. The authors concluded that the presence of Mn^{2+}_Sr ions is necessary but not sufficient to explain the multiglass behaviour in Mn-doped

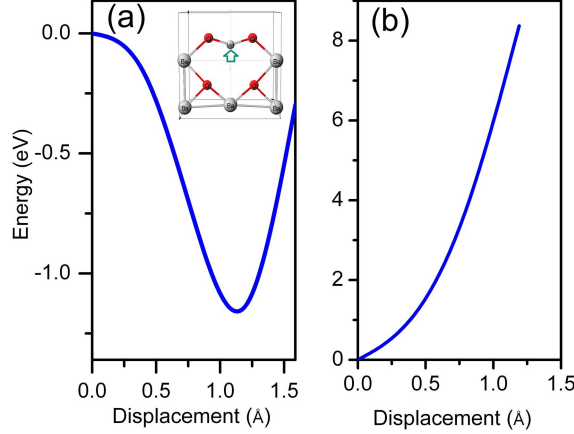


FIG. 1. Total energy dependence on the Mn (a) and Ba (b) displacements along the [001] direction in a $\text{Ba}_7\text{Ti}_8\text{MnO}_{24}$ supercell and pure BaTiO_3 , respectively. The insert shows the equilibrium position of the Mn atom in the (010) BaO plane.

SrTiO_3 ; the presence of $\text{Mn}_{\text{Ti}}^{4+}$ ions is also necessary.

Our calculations have been performed using a $2 \times 2 \times 2$ supercell (40 atoms plus vacancies). First, we replaced a Ti atom by a Mn ion to form a tetragonal $\text{BaTiO}_3\text{:Mn}$ structure with polarization axis along the z -direction. Then, we removed an oxygen atom to form a $\text{BaTiO}_3\text{:Mn-V}_\text{O}$ complex, a BaTiO_3 with a Mn impurity and an O vacancy. To study the effect of the vacancy position, we also have removed an oxygen atom along the x -axis.

We have performed computations with the ABINIT code.^{32,33} Norm-conserving pseudopotentials and Projector-Augmented Wave atomic data have been first generated with OPIUM and ATOMPAW codes, and then used along with the Wu-Cohen exchange and correlation functional.³⁴ A $4 \times 4 \times 4$ Monkhorst-Pack k -point grid has been exploited for the calculation of ground state properties. For the plane-wave expansion of the valence and conduction band wave-functions, a cutoff energy of 544 eV was chosen. To compare the effect of the large Coulombic repulsion between localized electrons, we have used LSDA and DFT+U approximations. In the latter, the Mn on-site Coulomb parameters, $U=8.0$ eV and $J = U/10$, were chosen. DFT+U calculations give somewhat larger ($\sim 5\%$) distance between the Mn ion and nearest O atom in the structures containing Mn-V complexes.

We first consider the case for a Mn impurity occupying the Ba site. In Fig. 1(a) we present the ground state energy as a function of the value of Mn shift along the [001] direction. All the other atoms are fixed in ideal perovskite positions. The curve has a

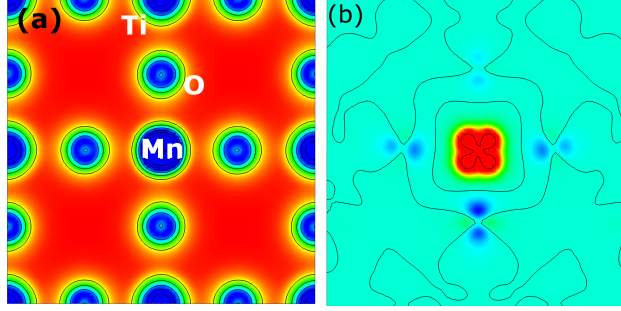


FIG. 2. (color online) The valence charge (a) and spin (b) densities around the Mn_{Ti} impurity in tetragonal BaTiO_3 in the plane parallel to the spontaneous polarization.

TABLE I. Interatomic distances, d , in pure tetragonal BaTiO_3 and with $\text{Mn}_{\text{Ti}}\text{-V}_\text{O}^z$ and $\text{Mn}_{\text{Ti}}\text{-V}_\text{O}^x$ defect complexes. Note that due to the breaking of cubic symmetry there are two kinds of apical (O_1 and O'_1) oxygen atoms with respect to the c -axis. In the presence of the V_O^x vacancy the tetragonal symmetry is also broken, so that two kinds of equatorial (two O_2 plus one O'_2) oxygen atoms can be distinguished. Labels are shown in Fig. 3. Results from LDA+U calculations are shown in square brackets.

d (Å)	pure BaTiO_3	with Mn-V_O^z	with Mn-V_O^x
$\text{Mn}(\text{Ti})\text{-O}_1$	2.234	2.013[2.069]	2.209[2.070]
$\text{Mn}(\text{Ti})\text{-O}'_1$	1.839	-	1.925[1.923]
$\text{Mn}(\text{Ti})\text{-O}_2$	1.989	2.049[2.108]	2.009[1.953]
$\text{Mn}(\text{Ti})\text{-O}'_2$	-	-	1.894[2.082]

minimum corresponding to 1.12 Å, which is twice as large as that found in SrTiO_3 .³⁰ The same displacement of Ba in pure BaTiO_3 , Fig. 1(b), leads to a steep rise in energy. Thus, the Mn impurity tends to be off-centered, like in SrTiO_3 .²⁸ Using DFT+U, we find that the Mn ion in the A site in the cubic structure has a magnetic moment of 5.1 μ_B . This indicates that Mn_{Ba} has a spin value of 5/2. This is in agreement with the experimental fact that in the incipient (cubic) ferroelectrics, like SrTiO_3 , Mn_A has a valency of 2+ and spin moment $S=5/2$.¹⁴ Decreasing U to ~ 4.0 eV reduces the computed moment to 4.5 μ_B . It is interesting that such a relatively high spin state of the Mn_{Ba} persists in going from the cubic to tetragonal phase, despite the fact that the atomic volume of the cubic phase is significantly lower (by 4 %) than that in the tetragonal phase. This situation is in contrast

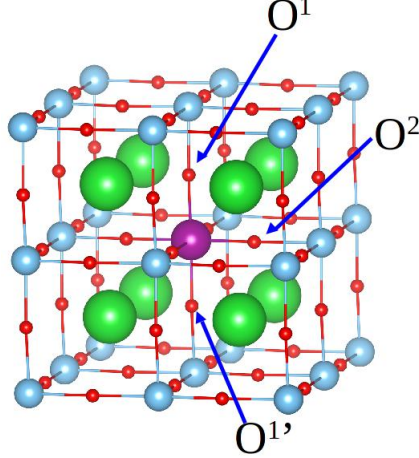


FIG. 3. (color online) Mn-doped BaTiO₃ structure. Arrows show two apical and one equatorial oxygen atoms, which are labeled as O₁, O₁' and O₂, respectively. Purple, red, blue and green balls correspond to Mn, Oxygen, Ti, and Barium atoms, respectively

to what occurs in MnO, where applied pressure induces magnetic collapse, as discussed in Ref. 35 and 36.

Mn in the B-site reduces c/a from 1.026 to 1.020. The Mn valence charge density is similar to the Ti, and the spin density is concentrated mostly on the Mn ion.(Fig. 2). The Mn magnetic moment is about $3.38 \mu_B$ with DFT+U, suggesting that the Mn_{Ti} ion has a high spin value of 3/2 and an oxidation state of 4+ in this case.

We also consider two types of Mn_{Ti}-V_O complexes containing two different kinds of nearest oxygen vacancies—V_O^z and V_O^x replacing the apical O¹ and equatorial O² oxygen atoms, respectively. The interatomic distances, d , in pure tetragonal BaTiO₃ and in the presence of such defects are listed in Table I. Fig. 3 shows the two apical and one equatorial oxygen atoms around Mn ion, which are labeled as O₁, O₁' and O₂, respectively. We found that when the complex Mn_{Ti}-V_O^z is introduced the tetragonal c/a is 1.020, the same as with Mn without a vacancy.

When the defect is oriented along the c -axis or polarization direction, the displacement of the Mn ion is reduced from that of the Ti atoms in pure BaTiO₃, as seen from Table I and Figs. 4(a) and (b). Valence charge densities for pure BaTiO₃ and BaTiO₃:Mn-V_O are shown in Figs. 4(c) and (d), respectively. There is practically no charge density at the oxygen vacancy. The spin density (Fig. 4(e)) is centered around the Mn defect as expected, but

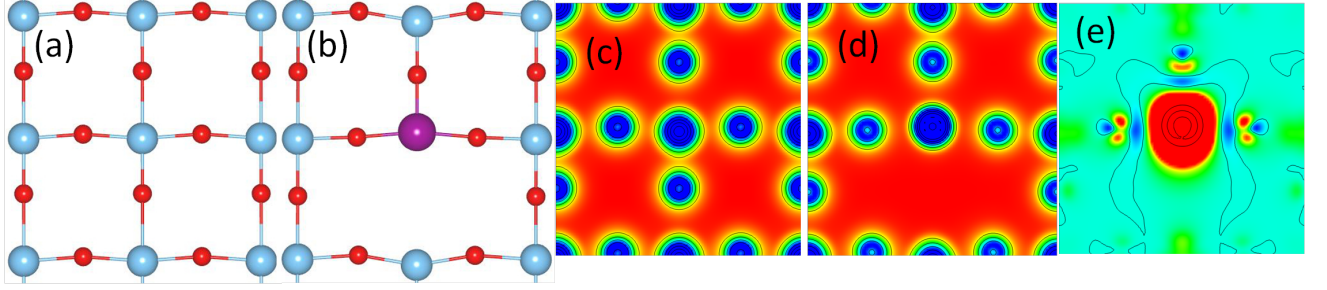


FIG. 4. (a) (color online) Undoped reference structure of BaTiO₃. (b) Mn_{Ti}-V_O defective associate oriented along the *c*-axis. Purple, red and blue balls correspond to Mn, Oxygen and Ti atoms, respectively. Note that Mn as a cation is displaced away from the oxygen vacancy due to electrostatic repulsive interaction. (c, d) Valence charge density for the structures (a) and (b). (e) Spin density for structure in (b), $\rho(r) \uparrow - \rho(r) \downarrow$.

overlaps with the neighboring O ions.

Our calculations show that in the Mn_{Ti}-V_O^z complex, the Mn magnetic moment is 4.93 μ_B indicating that the ion has a charge of 2+ with S=5/2. In the case of the Mn_{Ti}-V_O^x defects the Mn moment is about 4.9 μ_B consistent with a charge of 2+ and S=5/2. In both cases, the Mn ions maintain their valence states, their 3*d* shells are half-filled.

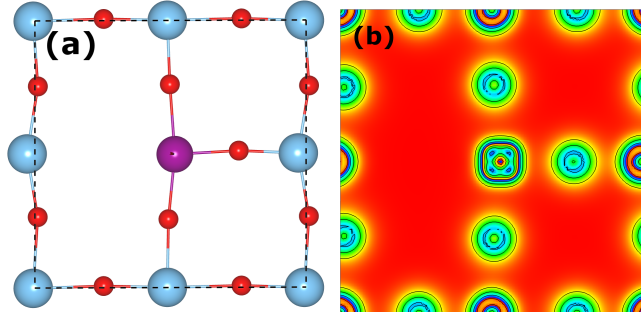


FIG. 5. (a) (color online) Mn_{Ti}-V_O^x defect with a vacancy occupying the nearest equatorial oxygen position. (b) The corresponding valence charge density.

When the vacancy occupies the nearest equatorial position relative to Mn, both the Mn and Ti atoms move away from the vacancy, see Table I and Fig. 5(a). Again, practically no charge density is detected on the vacancy position, see Fig. 5(b). Since this defect pair is oriented perpendicular to the spontaneous polarization, it is expected to affect the ferroelectricity to a lesser extent than when oriented along the *c*-axis.

Depending on the environment, Mn ions in BaTiO₃ can exist in the oxidation states Mn²⁺ and Mn⁴⁺ in agreement with the direct ESR experiments.¹¹ At the same time their magnetic moments can be either 3 to 5 μ_B . When a Mn impurity goes in the A site, the ratio c/a increases. When an Mn goes in the B site, c/a and the ferroelectric distortion decrease. The Mn oxygen vacancy complex with the oxygen vacancy on the c -axis is favored in energy. In particular, the V_O in the nearest apical position is favored by 0.10 eV as compared to the equatorial one. Therefore, the probability of finding an oxygen vacancy around the Mn center is highest along the the c -axis.

This work was supported by the Center the Office of Naval Research (ONR) grants grants N00014-12-1-1038 and N00014-14-1-0561 and the European Research Council Advanced Grant ToMCaT. Computations were performed on the DOD High Performance Computing Centers.

-
- ¹ E. Perez-Delfin, J. E. Garca, D. A. Ochoa, R. Prez, F. Guerrero, and J. A. Eiras, Journal of Applied Physics, **110**, 034106 (2011).
 - ² S. Wu, S. Wang, L. Chen, and X. Wang, Journal of Materials Science: Materials in Electronics, **19**, 505 (2008), ISSN 0957-4522.
 - ³ J.-H. Park, J. Park, J.-G. Park, B.-K. Kim, and Y. Kim, Journal of the European Ceramic Society, **21**, 1383 (2001), ISSN 0955-2219.
 - ⁴ M. A. Hentati, M. Guennou, H. Dammak, H. Khemakhem, and M. P. Thi, Journal of Applied Physics, **107**, (2010).
 - ⁵ H. Neumann and G. Arlt, *Ferroelectrics*, Ferroelectrics, **76**, 303 (1987), ISSN 0015-0193.
 - ⁶ G. Arlt and H. Neumann, *Ferroelectrics*, Ferroelectrics, **87**, 109 (1988), ISSN 0015-0193.
 - ⁷ X. Ren, Nat Mater, **3**, 91 (2004), ISSN 1476-1122.
 - ⁸ L. X. Zhang and X. Ren, Phys. Rev. B, **71**, 174108 (2005).
 - ⁹ L. Zhang and X. Ren, Phys. Rev. B, **73**, 094121 (2006).
 - ¹⁰ R. A. Serway, W. Berlinger, K. A. Mller, and R. W. Collins, Phys. Rev. B, **16**, 4761 (1977).
 - ¹¹ T. Kamiya, T. Suzuki, T. Tsurumi, and M. Daimon, Japanese Journal of Applied Physics, **31**, 3058 (1992), ISSN 1347-4065.
 - ¹² A. Tkach, P. M. Vilarinho, and A. L. Kholkin, Applied Physics Letters, **86**, (2005).

- ¹³ A. Tkach, P. Vilarinho, and A. Kholkin, *Acta Materialia*, **54**, 5385 (2006), ISSN 1359-6454.
- ¹⁴ V. V. Laguta, I. V. Kondakova, I. P. Bykov, M. D. Glinchuk, A. Tkach, P. M. Vilarinho, and L. Jastrabik, *Phys. Rev. B*, **76**, 054104 (2007).
- ¹⁵ W. Kleemann, V. V. Shvartsman, S. Bedanta, P. Borisov, A. Tkach, and P. M. Vilarinho, *Journal of Physics: Condensed Matter*, **20**, 434216 (2008), ISSN 0953-8984.
- ¹⁶ V. V. Shvartsman, S. Bedanta, P. Borisov, W. Kleemann, A. Tkach, and P. M. Vilarinho, *Phys. Rev. Lett.*, **101**, 165704 (2008).
- ¹⁷ W. Kleemann, S. Bedanta, P. Borisov, V. V. Shvartsman, S. Miga, J. Dec, A. Tkach, and P. M. Vilarinho, *The European Physical Journal B*, **71**, 407 (2009), ISSN 1434-6028.
- ¹⁸ H. Nakayama and H. Katayama-Yoshida, *Japanese Journal of Applied Physics*, **40**, L1355 (2001).
- ¹⁹ J. Lee, Z. Khim, Y. Park, D. Norton, N. Theodoropoulou, A. Hebard, J. Budai, L. Boatner, S. Pearton, and R. Wilson, *Proceedings of the 9th International Workshop on Oxide Electronics, Solid-State Electronics*, **47**, 2225 (2003), ISSN 0038-1101.
- ²⁰ Y. Shuai, S. Zhou, D. Brger, H. Reuther, I. Skorupa, V. John, M. Helm, and H. Schmidt, *Journal of Applied Physics*, **109**, (2011).
- ²¹ J. M. D. Coey, M. Venkatesan, and C. B. Fitzgerald, *Nat Mater*, **4**, 173 (2005), ISSN 1476-1122.
- ²² Y. Yao and H. Fu, *Phys. Rev. B*, **84**, 064112 (2011).
- ²³ E. Cockayne and B. P. Burton, *Phys. Rev. B*, **69**, 144116 (2004).
- ²⁴ L. He and D. Vanderbilt, *Phys. Rev. B*, **68**, 134103 (2003).
- ²⁵ H. Metri, R.-A. Eichel, T. Kloss, K.-P. Dinse, S. Laubach, S. Laubach, P. C. Schmidt, K. A. Schnau, M. Knapp, and H. Ehrenberg, *Phys. Rev. B*, **71**, 134109 (2005).
- ²⁶ R.-A. Eichel, P. Erhart, P. Trskelin, K. Albe, H. Kungl, and M. J. Hoffmann, *Phys. Rev. Lett.*, **100**, 095504 (2008).
- ²⁷ Z. Zhang, P. Wu, L. Lu, and C. Shu, *Applied Physics Letters*, **92**, (2008).
- ²⁸ O. Kvyatkovski, *Physics of the Solid State*, **51**, 982 (2009), ISSN 1063-7834.
- ²⁹ O. Kvyatkovskii, *Physics of the Solid State*, **54**, 1397 (2012), ISSN 1063-7834.
- ³⁰ I. V. Kondakova, R. O. Kuzian, L. Raymond, R. Hayn, and V. V. Laguta, *Phys. Rev. B*, **79**, 134117 (2009).
- ³¹ R. O. Kuzian, V. V. Laguta, A.-M. Dar, I. V. Kondakova, M. Marysko, L. Raymond, E. P. Garmash, V. N. Pavlikov, A. Tkach, P. M. Vilarinho, and R. Hayn, *EPL (Europhysics Letters)*,

- 92**, 17007 (2010), ISSN 0295-5075.
- ³² G. Xavier, “A brief introduction to the abinit software package,” (2009).
- ³³ X. Gonze, B. Amadon, P.-M. Anglade, J.-M. Beuken, F. Bottin, P. Boulanger, F. Bruneval, D. Caliste, R. Caracas, M. Ct, T. Deutsch, L. Genovese, P. Ghosez, M. Giantomassi, S. Goedecker, D. Hamann, P. Hermet, F. Jollet, G. Jomard, S. Leroux, M. Mancini, S. Mazevet, M. Oliveira, G. Onida, Y. Pouillon, T. Rangel, G.-M. Rignanese, D. Sangalli, R. Shaltaf, M. Torrent, M. Verstraete, G. Zerah, and J. Zwanziger, *40 YEARS OF CPC: A celebratory issue focused on quality software for high performance, grid and novel computing architectures*, Computer Physics Communications, **180**, 2582 (2009), ISSN 0010-4655.
- ³⁴ Z. Wu and R. E. Cohen, Phys. Rev. B, **73**, 235116 (2006).
- ³⁵ R. E. Cohen, I. I. Mazin, and D. G. Isaak, Science, **275**, 654 (1997).
- ³⁶ J. Kunes, A. V. Lukoyanov, V. I. Anisimov, R. T. Scalettar, and W. E. Pickett, Nat Mater, **7**, 198 (2008), ISSN 1476-1122.